Fuel Processing Technology, Vol. 167, December 2017, pp. 314-321
DOI:10.1016/j.fuproc.2017.07.015

SO_3 formation and the effect of fly ash in a bubbling fluidised bed under oxy-fuel combustion conditions

*Yerbol Sarbassov[a], Lunbo Duan[b], Michal Jeremias[c], Vasilije Manovic[a], Edward J. Anthony[a,]**

[a]*Combustion and CCS Centre, Cranfield University, Cranfield MK43 OAL, United Kingdom;*

[b]*School of Energy and Environment, Southeast University, 2 Sipailou, Nanjing, 210096, P. R. China;*

[c]*Institute of Chemical Process Fundamentals of the Czech Academy of Sciences of the Czech Republic, Rozvojova 135, 165 02, Praha 6 - Suchdol, Czech Republic,*

Corresponding author: Edward J. Anthony; Combustion and CCS Centre, Bedford MK43 0AL, Bedfordshire, UK. E-mail: b.j.anthony@cranfield.ac.uk

Abstract

This study investigates SO_3 formation under air-fired and oxy-fuel combustion environments in a bench-scale bubbling fluidised bed. Flue gas compositions typical of air-fired and oxy-fuel environments were simulated with synthetic gas mixtures. Parameters such as bed temperature and SO_2 and H_2O concentrations were varied to determine their effect on the formation of SO_3. Tests were also performed using three fly ashes produced from three different coals and combustion systems. Oxy-fuel combustion always led to increased SO_3 concentration as compared to typical air-fired environments. SO_3 concentrations increased with combustion temperature and O_2 concentrations. SO_3 formation also depends on the chemical composition of the fly ash.

Keywords: SO_3 formation, catalysis, oxy-fuel combustion, fluidised bed.

Published by Elsevier. This is the Author Accepted Manuscript issued with:
Creative Commons Attribution Non-Commercial No Derivatives License (CC:BY:NC:ND 4.0).
The final published version (version of record) is available online at DOI:10.1016/j.fuproc.2017.07.015
Please refer to any applicable publisher terms of use.

1. Introduction

Oxy-fuel combustion is an emerging energy technology which facilitates carbon capture and storage (CCS), where the fuel is burned in a mixture of oxygen and recycled flue gas (RFG*)* to produce a nearly pure stream of CO_2 and steam [1,2]. The RFG allows the combustion temperature and heat transfer profile in the boiler to be kept at levels similar to air-fired combustion conditions [1,3], but the concentrations of SO_2, NO_x and H_2O are several times higher due to the RFG [4]. As an example, SO_2 concentrations in oxy-fuel combustion can be 3 to 4 times higher than in air-fired combustion [5-6]. The increase in SO_2, O_2 and H_2O concentrations can be expected to enhance SO_3 formation. This in turn will increase the dew point, which potentially can lead to serious operational problems due to corrosion downstream of the boilers [7-8]. Currently, an increase of the flue gas temperature appears to be the most practical approach to avoid sulphuric acid deposition on downstream surfaces, albeit with a resulting decreased boiler efficiency [7]. Moser [7] suggests that an increase of flue gas temperature by 1.7°C within the air heater results in a decrease of 1% in the unit heat rate. Annually, the benefit derived from SO_3 removal and subsequent corrosion reduction exceeds $1000 per 1 MW of generated electricity based on estimates for a 500 MW power plant [7]. Thus, there are financial incentives to understand the effect of recycled SO_2 and H_2O on the formation of SO_3.

SO_3/SO_2 conversion in typical coal-fired plants can vary from 1 to 5% [9]. These values depend on numerous parameters including the sulphur content in the fuel, flame temperature and chemical composition of the fly ash (FA) [9]. SO_3 produced can be adsorbed or its formation enhanced by the fly ash components, depending on the minerals present in the ash such as those of alkali and alkaline earth metals or species like Fe_2O_3. The primary formation of SO_3 is due to oxygen radicals in the combustor post-flame zone [10]. In a pulverised coal-fired boiler this happens at temperatures higher than 900°C (as indicated by reaction (1), where M is a third body) [11]:

$$SO_2 + O\ (+M) \rightleftharpoons SO_3\ (+M) \tag{1}$$

Secondary SO_3 formation occurs via the production of $HOSO_2$ radicals, which react to form HO_2 radicals and SO_3:

$$SO_2 + OH\ (+M) \rightleftharpoons HOSO_2\ (+M) \tag{2}$$

$$HOSO_2 + O_2 \rightleftharpoons SO_3 + HO_2 \tag{3}$$

This process is more important at temperatures below 700°C, due to the low thermal stability of $HOSO_2$ [12].

The results of SO_3 formation tests in bench-scale facilities under air- and oxy-fuel-fired conditions are summarised in Table 1.

Table 1

SO_3 formation in quartz tube flow reactors

Size (D x L mm)	Temp. (ºC)	Inlet gas composition	Residence time (s)	SO_3/SO_2 ratio (%)	Reference
25.4 x 610	1030-1530	Air + 0.7% SO_2	5.5-5.7	0.2	[13]
14 x 1829	500-900	Air (+ H_2O-8%), SO_2 (0.14%)	0.9-9.6	0.36-4.8	[14]
10 x 450	850-1066	SO_2 (0.55%); O_2 (0-0.21%); bal-N_2	Up to 6	0.36	[11]
12 x 250	400-1000	Mixture (SO_2-0.1%, H_2O-3%, O_2-5%, bal-N_2)	0.3-0.9	0.14-0.77	[15]
50 x 900	527-1400	SO_2-0.1%, O_2-3%, H_2O-1.11%, bal-N_2/CO_2	Up to 5	0.1-1.7	[16]
15.5 x 1115 (420)[a]	400-700	O_2-6%, SO_2 - 0.3%, H_2O, bal-N_2/CO_2	1.5	0.1-1.5	[17]
50 x 1500	350-1050	O_2-5%, SO_2-0.05, 0.15, 0.25%, H_2O-0.03%, bal-CO_2	N/S[b]	(0.05%)[c] 0.11 (0.15%)[c] 0.16 (0.25%)[c] 0.21	[18]

Fleig et al. [16] measured SO_3 in a bench-scale quartz tube reactor and modelled homogeneous gas-phase reactions. Their results suggest a significant increase in SO_3 formation due to the higher H_2O and O_2 concentrations under oxy-fuel combustion conditions. Belo et al. [15] investigated the catalytic effect of fly ash on SO_3 formation in a horizontal tube furnace. They stated that the catalytic effect of Fe_2O_3 was greatest at 700°C and decreased gradually at lower and higher temperatures, but they found no effect of H_2O on SO_3 formation. Duan et al. [17] investigated the formation of SO_3 in an oxy-fired 50 kW circulating fluidised bed (CFB) unit and in a fixed bed rig. They tested the effects of two different ashes and three metal oxides (Fe_2O_3, CuO and V_2O_5) as catalysts in a fixed bed [17]. The results showed that SO_3 concentrations were 4.5 times higher in the oxy-fuel CFB tests, while the fixed bed tests revealed the strong catalytic effect of V_2O_5. According to recent tests by Wang et al. [18], higher H_2O concentrations (over 15%) inhibit SO_3 formation.

[a] Only 420 mm of total length is heated

[b] Not specified (N/S). Based on size of tube and flow rate, calculation shows long residence time for this work

[c] SO_2 concentrations (vol. %)

SO_3 emissions in pilot-scale units under oxy-fuel combustion were also investigated by Ahn et al. [19] in a 1.5 MW pulverised coal (PC) combustor and 0.3 MW CFB unit. Here, SO_3 emission were 4 to 6 times higher under oxy-fuel combustion conditions than air combustion conditions when high-sulphur coal (~4% S) was burned. Sporl et al. [20] also measured SO_3 concentrations in a 0.5 MW oxy-PC combustor and explored the effects of electrostatic precipitator (ESP) and selective catalytic reduction (SCR) units on the formation of SO_3. They concluded that ~62% of SO_3 capture occurred in the SCR unit in the oxy-fuel combustion mode [21]. Fleig et al. [22] conducted tests in a 0.1 MW oxy-PC unit, burning propane doped with sulphur, and also studied the effect of wet and dry RFG and observed higher SO_3 concentrations in wet tests than in the dry RFG tests, indicating enhanced formation of SO_3 due to the presence of H_2O [22].

Only limited experiments can be found in the literature on SO_3 formation in oxy-fired bubbling fluidised beds (BFBs) [17,19,23]. Moreover, there are relatively few studies on the effects of fly ash on SO_3 formation [15,17, 24]. Therefore, further investigation of both the sand and “fly ash-catalysed” formation of SO_3 is desirable to better understand SO_3 formation mechanisms in oxy-fired FBC. The effect of silica sand on SO_3 formation was investigated by Dennis and Hayhurst [25], who concluded that SO_3 was mainly produced on the surface of the sand via a heterogeneous catalytic effect between the temperatures of 700-1000°C [25]. Therefore, it is important to compare the catalytic effect of sand vs. fly ash at higher temperatures and determine whether sand has a catalytic effect at lower temperatures.

2. Experimental Methodology

2.1. Bubbling fluidised bed

A schematic diagram of the bench-scale BFB rig is provided in Fig. 1. The reactor consists of inner and outer stainless steel tubes, gas lines for O_2, CO_2, SO_2, and N_2, water pump, and electrically-heated furnace. Solids can be introduced by means of a feeding port at the head of the reactor. At the hot exit line, a sintered filter is installed for particulates removal. The inner diameter (ID) of the inner tube is 25 mm and its height is 550 mm. The outer tube has an ID of 38 mm and a height of 1180 mm. The distributor plate consists of 4 layers of stainless steel (316) mesh clamped with an open cap to the bottom part of the inner tube. The reactor temperature was measured by a K-type thermocouple and the pressure drop (ΔP) across the bed was measured by pressure transducers. All readings were recorded by a Picolog data acquisition system. The mixtures of gases and H_2O were fed to the bottom part of the outer tube to pass through the pre-heating section. The flow rate of gases to the reactor was controlled by mass flow controllers (MFC-Bronkhorst). Deionised water was fed by a high-pressure pump and supplied to the pre-heated section of the outer tube to avoid steam condensation in the bottom section of the reactor. After passing through the main heated section of the reactor, the exit gas composition was measured by a Fourier transform infra-red analyser (FTIR, Protea, model FTPA-002).

A thumb-type sintered filter with a maximum pore size of 60 μm was placed at the

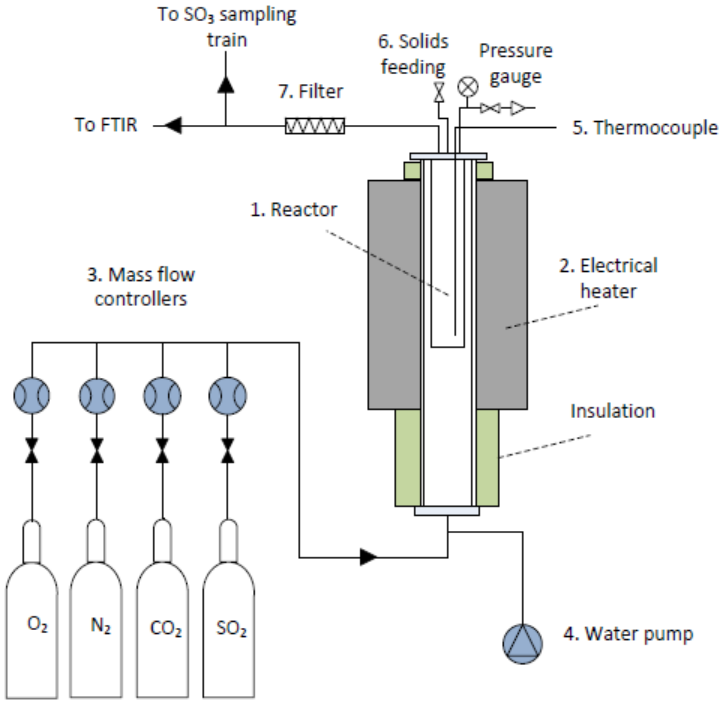


Fig. 1. Bench-scale bubbling fluidised bed

reactor exit to prevent elutriation. All tubes in the exhaust section were made of stainless steel. The tube for exit gases had an ID of 4.2 mm and height of 700 mm. The smaller diameter pipe was used to prevent SO_3 loss in the sampling line by reducing the residence time of the gas leaving the reactor and entering the sampling train. The residence time of the exit gas in the exhaust section was less than 1 s. According to the studies of Lindsay and Flint [14], SO_3 capture by the tube wall can be minimised if a short residence time is ensured in the sample lines to the SO_3 analytical train. A similar approach for such measurements was used by Dennis and Hayhurst [25]. Moreover, the whole length of the gas sampling line was heated with a string heating element and maintained at a temperature of 290-300°C and the exit gas temperature was maintained at 185 to 190°C. Another reason for maintaining the heater at such high temperatures is to avoid the formation of aerosols in the quartz filter fitted in the SO_3 sampling train [26].

2 Materials

In this study silica sand with a mean particle size of 260 μm is used as a fluidised–bed (FB) material. In addition, three different fly ashes were used in the BFB to investigate the catalytic effect of minerals on the formation of SO_3. Fly ashes were supplied by CanmetENERGY (Canada), a British power plant (UK) and Southeast University (China). Here, the fly ashes are referred to as Canadian, British and Chinese, respectively. The last fly ash was produced from a 50 kW oxy-fired CFB unit located at Southeast University. Further details about the coals and the combustion units themselves can be found elsewhere [27]. XRF analysis of the fly ashes as received is given in Table 2. The Canadian ash has a very high CaO content, and the British ash a very low one, but all of the ashes have a Ca/S molar ratio above 4, meaning that they can capture some SO_2/SO_3, and at the end of the experiment, Ca/S molar ratios ranged from 2.4 (British fly ash), and below indicated that some SO_2 capture had taken place.

The particle sizes of the fly ashes used in this work were sieved to be normally between 90 and 212 μm, with a mean particle diameter (d_p) of 150 μm. However, a larger particle size was used for the Chinese fly ash, as shown in Fig. 2(b). Four layers of fine metal mesh with a maximum pore size of 75 and 120 μm were used to

Table 2

Chemical composition of fly ashes (wt. %)

Fly ash source	SiO_2	Al_2O_3	Fe_2O_3	CaO	MgO	Na_2O	K_2O	TiO_2	P_2O_5	SO_3
Canadian	25.44	9.12	8.59	29.95	9.02	0.20	0.78	0.21	0.11	9.46
British	48.00	29.50	9.00	3.00	2.50	1.25	3.00	0.95	-	0.80
Chinese	45.12	34.14	4.16	8.66	1.36	0.46	0.99	1.53	0.09	3.06

keep solids in the reactor. The particle size distribution (PSD) of solids is shown in Fig. 2.

For the SO_3 analysis, a solution containing 1.95 g of barium perchlorate trihydrate (99.9%-Ba, CAS: 10294-39-0; Stream Chemicals, Newburyport, MA 01950, USA) was dissolved in 200 mL of de-ionised water at room temperature. Then, 800 mL of pure iso-propanol was added to make 1000 mL of barium standard solution. The solution was stored in a 1 L glass bottle at room temperature. The solution is stable for up to two weeks. For the SO_2 measurements, two bottles were filled with 100 mL of solution containing 3% hydrogen peroxide, and one with 100 mL of de-ionised water. The fourth bottle was filled with silica gel. All 4 bottles were maintained in a

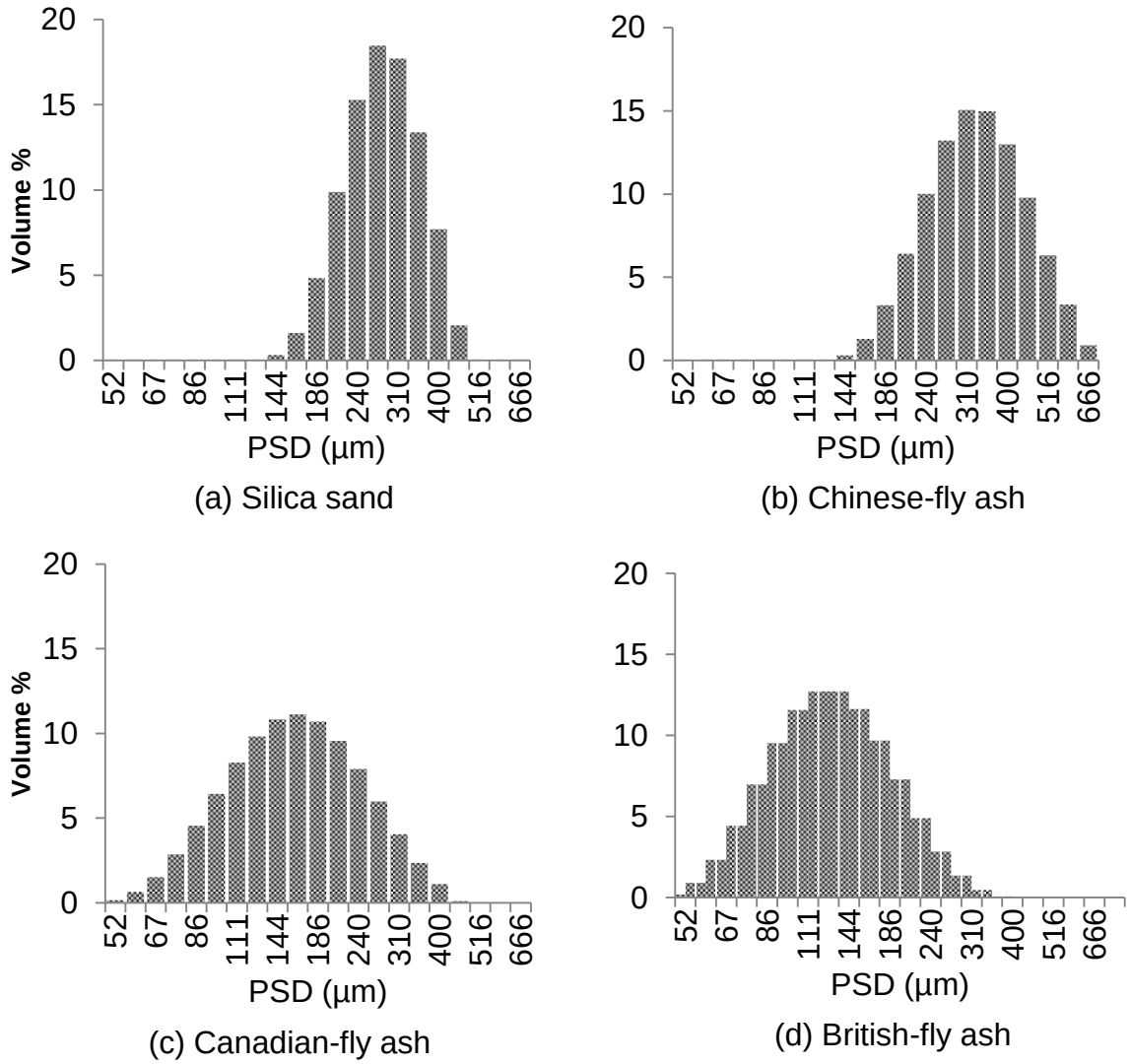


Fig. 2. Particle size distribution of bed solids

water bath at a temperature below 5°C by adding fresh ice during the test. The temperature in the water bath was monitored by a K-type thermocouple.

2.2 Experimental procedure

A factorial approach was chosen for the experimental design with lower and higher values for SO_2 concentrations and bed temperatures (T_{bed}) as shown in Table 3. SO_2 concentrations of 1000 and 4000 ppm were used to simulate average and high-sulphur coal combustion flue gases in the BFB. The 4000-ppm SO_2 content represents high-sulphur coal combustion in an oxy-fuel combustion environment with wet RFG. As discussed above, the wet RFG in oxy-fuel combustion increases steam content in the combustion furnace [4]. This was achieved in these tests by increasing the steam content in the reactor from 6% to 11% by volume (Table 4). Here, low-temperature (400°C) tests represent the formation of SO_3 at the back end of the combustion furnace, while the higher-temperature case (950°C) represents the environment in the fluidised bed. Reactant gases were supplied by cylinders and metered by mass flow controllers.

Table 3

Experimental conditions of SO_3 formation tests

Test parameters:	**Lower Value**	**Higher Value**
Operating temperature (T_{bed}), °C	400	950
SO_2 inlet, ppm	1000	4000
Flow rate, L/min	2.6	1.4
Sampling volume (EPA[d]), L	300	300
Sampling time, h	1.9	3.9

Table 4

Inlet mixture composition (by volume, wet basis)

Test run	Mode	Temp (°C)	SO_2 (ppm)	O_2 (%)	H_2O (%)	N_2 (%)	CO_2 (%)
1	Air	400	1000	4	6	Balance	15
2	Air	400	4000	4	6	Balance	15
3	Air	950	1000	4	6	Balance	15
4	Air	950	4000	4	6	Balance	15
5	Oxy	400	1000	5	11	0	Balance
6	Oxy	400	4000	5	11	0	Balance
7	Oxy	950	1000	5	11	0	Balance
8	Oxy	950	4000	5	11	0	Balance

[d] EPA protocol on measuring sulphur trioxide and sulphur dioxide emissions

The flue gas compositions for these tests are shown in Table 4. These tests can be designated as:

- *Sand tests:* The conversion of SO_2 to SO_3 tests were performed in the presence of 20 g of washed and sieved silica sand.
- *Fly ash tests:* The conversion of SO_2 to SO_3 tests were conducted in the presence of 20 g of silica sand and 10 g of fly ash.

Prior to starting each test, all exit gas tubes and metal connections were checked for leakage. The reactor was heated at a rate of 20°C/min to reach the desired temperature. 20 g of silica sand was introduced into the reactor when the set temperature was reached. Once the steady-state condition was achieved as determined by FTIR, the exit lines were connected to the SO_3 sampling line. At typical fluidising conditions (20°C and 100 kPa), the volumetric flow rate was 2.6 L/min at 400°C and 1.4 L/min at 950°C, to maintain a similar superficial gas velocity in the reactor. The residence time in the reactor was ~3 s under actual conditions, which is equivalent to a fluidisation velocity (U/U_{mf}) of around 3.8. The minimum fluidisation velocity (U_{mf}) was calculated using the Wen and Yu correlation [28]. The apparent density of bed materials was determined by the water displacement method. The apparent density of silica sand was 2500 kg/m^3, while for Canadian fly ash it was 950 kg/m^3 and ~750 kg/m^3 for both the British and Chinese fly ashes. Tests with the Canadian and British fly ash were performed twice to ensure repeatability, while experiments with Chinese fly ash were limited to one condition, namely 950°C and 1000 ppm of SO_2.

Ash characterisation: A thermogravimetric analyser (TGA, model Q500, TA Instruments, Inc.) was used to determine the amount of unburnt carbon in the ash. The tests were done with air and inert, and the mass change with temperature up to 900°C was measured.

2.3 SO_3 measurements

The controlled condensation method (CCM) which is based on the EPA method 8A was chosen to measure SO_3 concentrations as it is the most common method for measuring SO_3 [29-30]. Due to the size limitations of the rig, the total sampling flow rate of exit gas was several times lower than that recommended by the EPA method. Therefore, the sampling time was extended to match a minimum gas volume of 300 L. At 950°C, the duration of sampling was around 4 h, while only 2 h was required at 400°C. The SO_3 sampling train is shown in Fig. 3. The sampling probe for the exit gas is connected to the quartz tube and sealed with a high-temperature ceramic

paste. The exit gas is additionally filtered in the glass sampling train by a quartz filter and paper. The quartz filter had a maximum pore size of 100 µm.

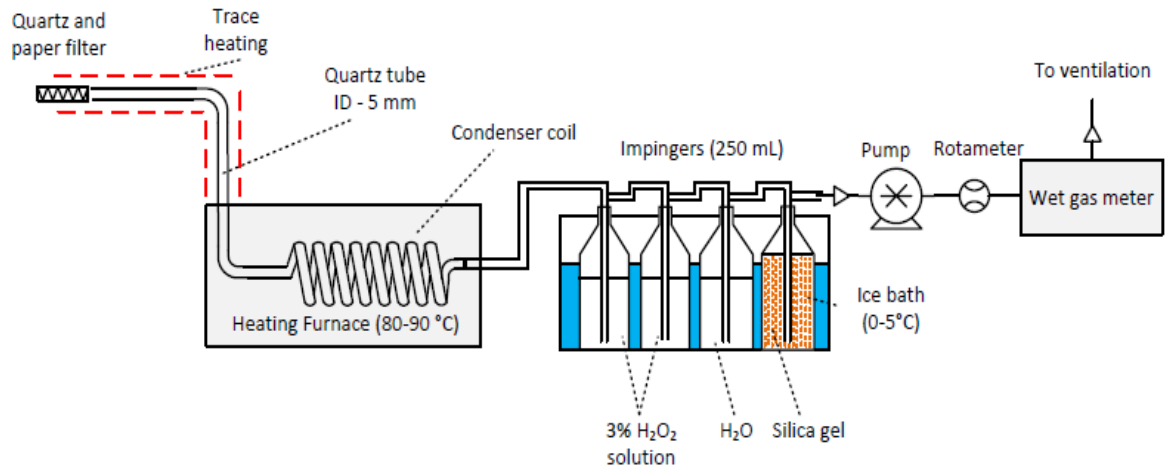


Fig. 3. SO_3 sampling train is based on EPA method 8A

The paper filter is required to remove fine particles from the gas stream as they can result in positive errors. The probe and filter are maintained at 290-300°C to avoid the formation of aerosols. After passing the filter, the sampling gas undergoes a temperature drop in the glass condenser which is maintained at 80 to 90°C. At this temperature, SO_3 in the exit gas can be expected to condense on the glass wall of the condenser. The remaining gas passes through 3% hydrogen peroxide solution; here any SO_2 is converted to sulphuric acid, even at low temperature. The residual gas moisture is removed by silica gel and the gas then goes to a wet gas meter (WGM). A calibrated WGM was used in this test to avoid flow measurement errors, and was fixed in a horizontal plate and positioned by a spirit level. The top of the water level was monitored in the WGM. The glass condenser, probe and first two impingers were titrated separately using a barium perchlorate trihydrate solution.

2.4 Pressure-drop measurements

Pressure-drop profiles at 400°C and 950°C are illustrated in Fig 4 and 5, respectively. It can be seen from Fig. 4 that feeding 20 g of silica sand increased ΔP across the bed to 0.36–0.40 kPa. An addition of 10 g of ash particles increased ΔP further to

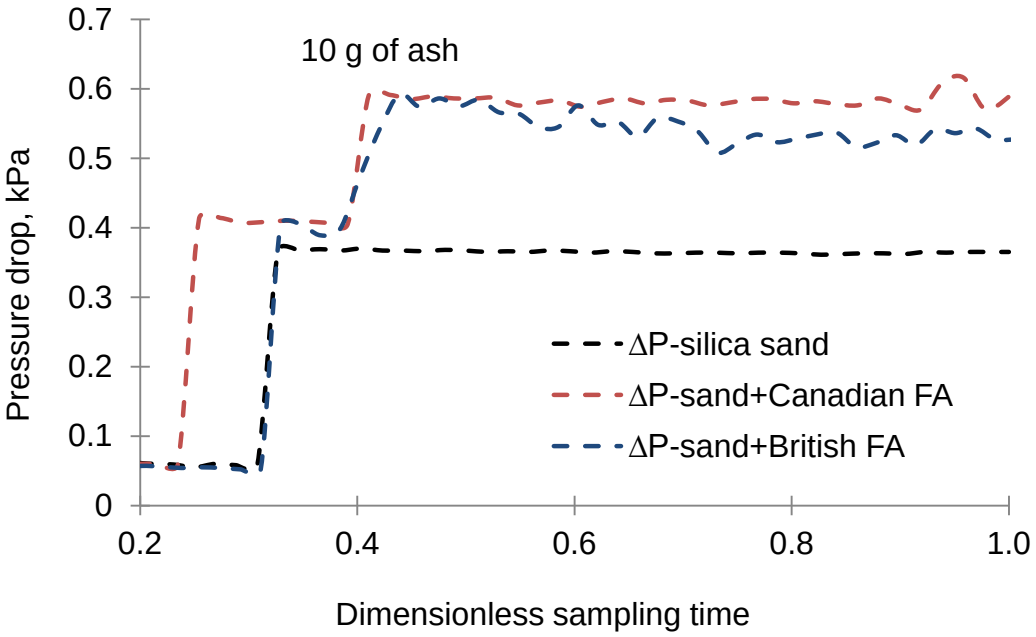


Fig. 4. Pressure-drop measurements at 400°C

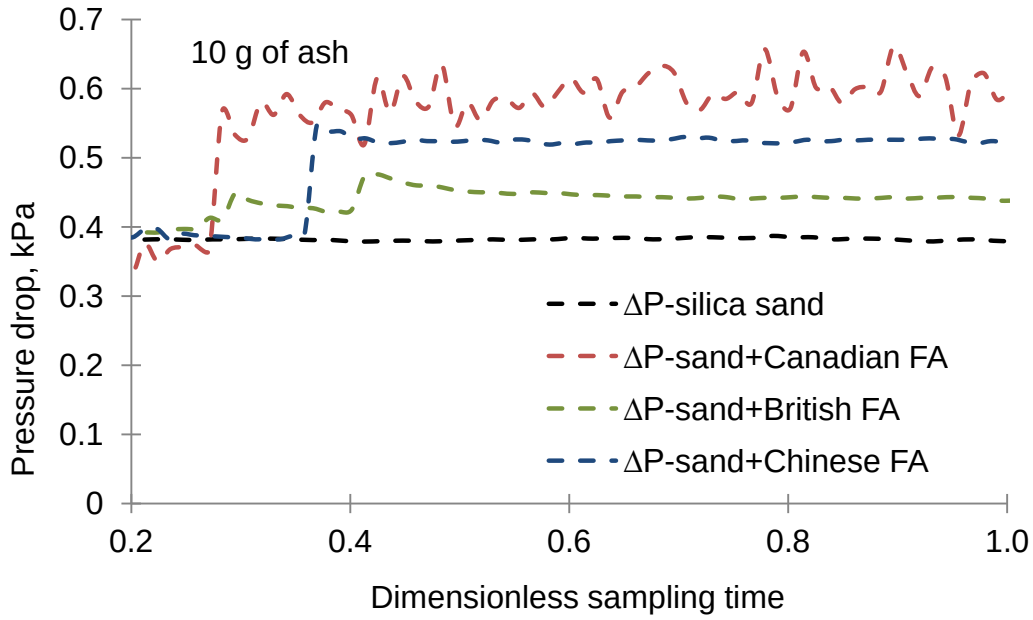


Fig. 5. Pressure-drop measurements at 950°C

0.55–0.59 kPa. The ΔP during the heating stage was between 0.01 and 0.05 kPa in the empty reactor. This ΔP was due to the resistance of the distributor plate. A fluctuation in ΔP profiles was also noted with ash tests. This could be due to the adjustable vacuum pump for SO_3 sampling. A gradual decrease of ΔP profiles was noted in the tests with British fly ash. This could be explained by the lower density of ash particles that were elutriated from the reactor and remained in the sintered filter. Similar ΔP profiles were observed for the test carried out at 950°C. The repeated fluctuation of ΔP in the test with British fly ash at 950°C appears to be a result of the split feed of ash.

However, ΔP for the British and Chinese ashes decreased noticeably after feeding at 950°C. This change of ΔP could be explained by the loss of unburnt carbon content in the ash. In order to confirm this, ash particles were tested in the TGA under air and inert gas and heated up to 900°C. The Chinese ash had the highest content of unburnt carbon, as the mass of the sample dropped by 30%. The values for British and Canadian ashes were 16% and 7%, respectively. The high level of unburnt carbon in the Chinese ash is likely due to the short residence time in the pilot-scale oxy-CFB unit [17]. Here, the ΔP profile with Canadian ash was more stable compared to that of the British and Chinese fly ashes. The mass change curves in

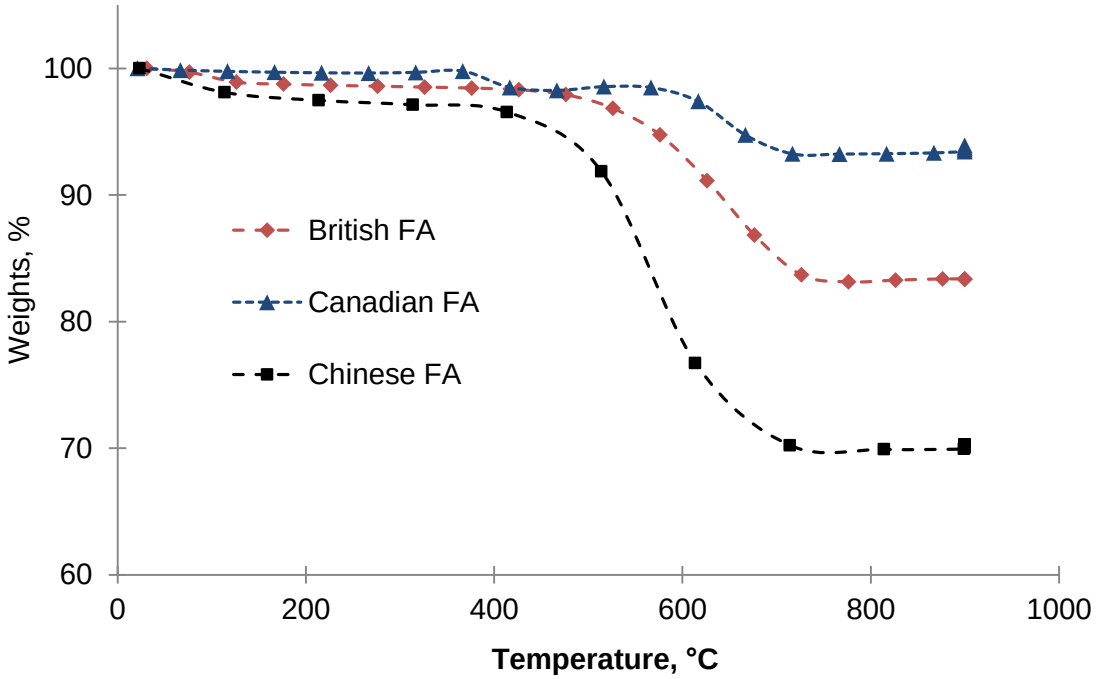


Fig. 6. TGA test of FAs under air-fired conditions

the TGA provided a reasonable explanation of the ΔP profiles observed in the BFB tests.

3 Results and Discussion

3.1 Uncatalysed SO_3 formation

3.1.1 Thermodynamic equilibrium of SO_3/SO_2 conversion

The thermodynamic equilibrium curves of SO_3/SO_2 conversion were evaluated with an online calculator developed by Colorado State University [31]. Gas compositions typical for flue gas from air and oxy-fired conditions were selected as seen in Fig. 7. A SO_2 level of 1000 ppm was chosen for the purposes of calculation. In the current simulation, SO_3/SO_2 conversion was effectively 100% at 400°C and 4.6% at 950°C.

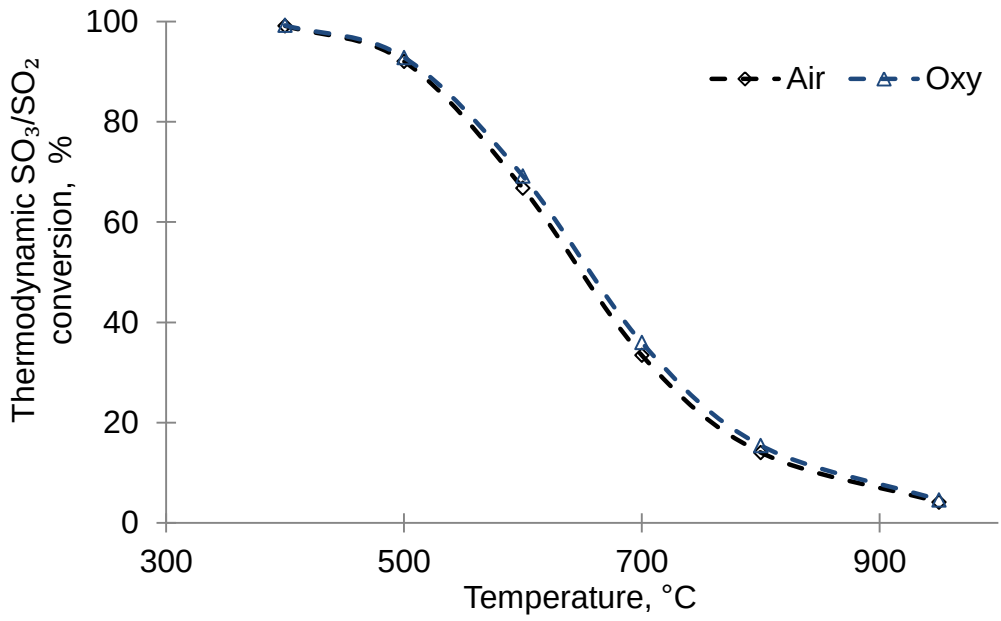


Fig. 7. Thermodynamic equilibrium SO_3/SO_2 conversion:
Air: SO_2-1000 ppm, O_2-4%, CO_2-15%, H_2O-6%, N_2-Balance; Oxy: SO_2-1000 ppm, O_2-5%, H_2O-11%, CO_2-Balance)

3.1.2 Effect of bed temperature

The effect of bed temperature on SO_3/SO_2 conversion is shown in Fig. 8 together with referenced values. The SO_3/SO_2 ratio at 400°C is very low and is in the range of 0.1% for both SO_2 concentration levels. The SO_3/SO_2 conversion increased with temperature presumably because of kinetic effects. The SO_3/SO_2 conversion at 950°C was 1.8% and 2.2%, with SO_2 of 1000 ppm and 4000 ppm, respectively. In the SO_3 formation studies conducted by Duan et al. [17], this value was 0.12% at 400°C and increased gradually to 0.18% at 700°C. In the temperature range of 400 to 1000°C, Belo et al. [15] produced an exponential type curve for SO_3/SO_2 conversion by using the kinetic model of Burdett et al. [11]. It can therefore be concluded that the formation of SO_3 is kinetically favoured at relatively higher temperatures close to 700°C. In this connection, it is worth noting that Lindsay and

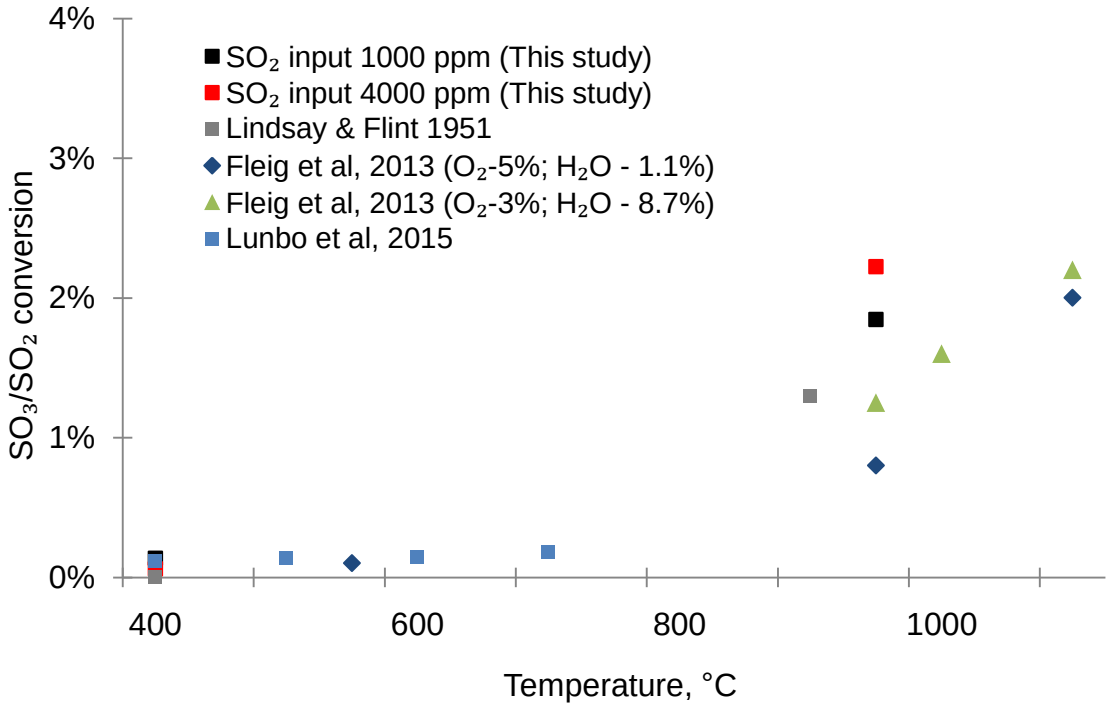


Fig. 8. SO_3/SO_2 conversion compared with the literature

Flint [14] concluded that the formation of SO_3 in the absence of catalysis at low temperatures is negligible. Similar observations were made by Fleig et al. [16] for temperatures near or below 500°C. They studied SO_3 formation in the temperature range of 423 to 1400°C in a heated vertical tube reactor using different flue gas compositions, as shown in Fig. 8. It can be concluded that the SO_3/SO_2 conversion starts to approach thermodynamic equilibrium at temperatures higher than 800°C. At lower temperatures, in the absence of catalysis the kinetics of SO_3 formation are too slow to result in a significant effect on SO_3 concentrations.

3.1.3 Effect of SO_2 concentrations

The effect of SO_2 concentrations on SO_3 formation is shown in Fig. 9. This effect at 400°C was more pronounced under air-fired gas composition where SO_3 concentrations increased from 1.6 to 2.2 ppm, while under oxy-fuel conditions it increased from 0.5 to 0.9 ppm at both SO_2 concentrations. Very little difference was noted in terms of SO_3 concentrations between air and oxy-firing conditions for tests at 400ºC. However, in agreement with the literature, the results for SO_3 formation at 400°C showed a slight increase with SO_2 concentrations [18-19]. There was also no significant effect of H_2O at 400°C. At 950°C, SO_3 concentrations under oxy conditions were higher than for the test under air-fired conditions for 1000 ppm of SO_2, see Fig.9 (b). In the case with high SO_2 content of 4000 ppm, 81 ppm of SO_3 was measured in the air-fired case, while only 29 ppm of SO_3 was seen in the oxy-

fuel environment. The 81 ppm of SO_3 concentration in Fig. 9(b) seen for air environment and 4000 ppm of SO_2 test was comparable with other studies at higher temperatures (see **Error! Reference source not found.**). It can be seen that the O_2/SO_3 conversion here was 2.2%, which is only slightly higher than the SO_3 concentration measured by Fleig et al. [16]. However, it is clear that SO_3 formation increases with increased SO_2 concentrations as would be expected at both 400 and 950°C.

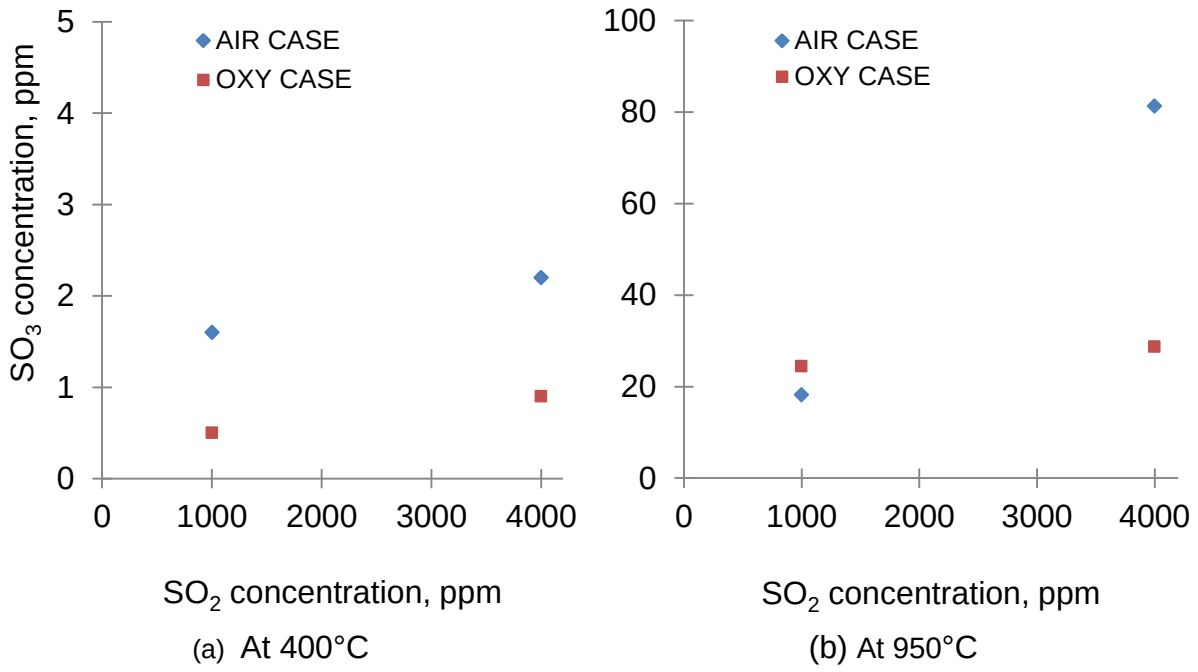


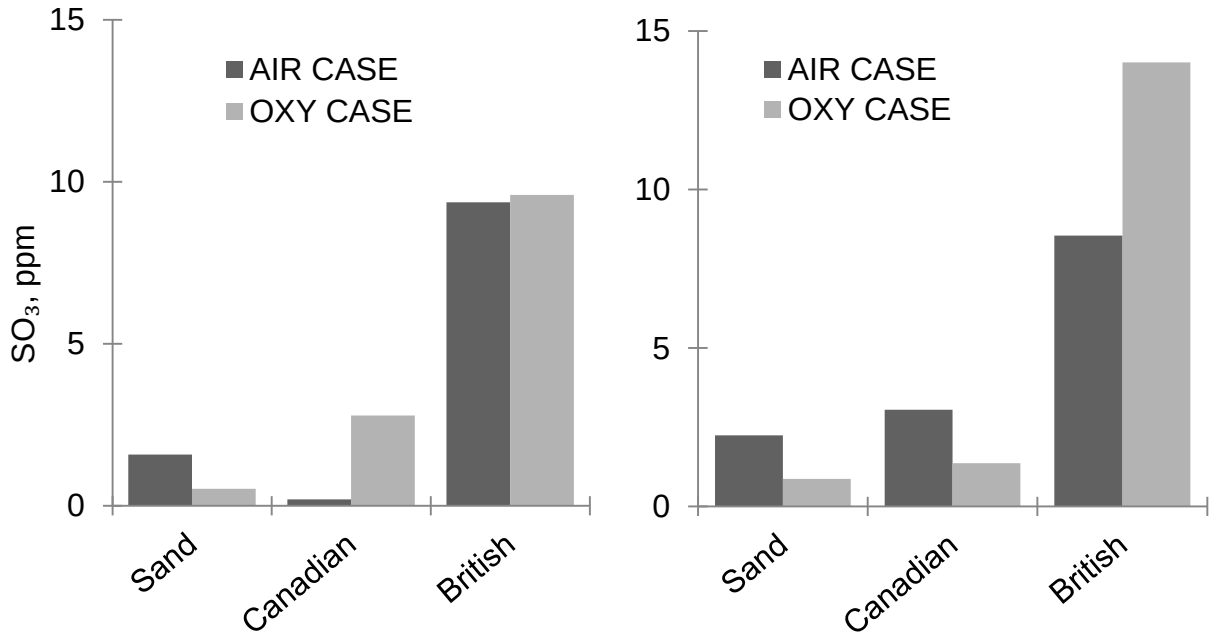
Fig. 9. Effect of SO_2 concentration at 400 and 950 °C

(Air: O_2-4%, CO_2-17%, H_2O-6%, Balance-N_2; Oxy: O_2-5%, H_2O-11%, Balance-CO_2)

3.2 Fly ash-catalysed SO_3 formation

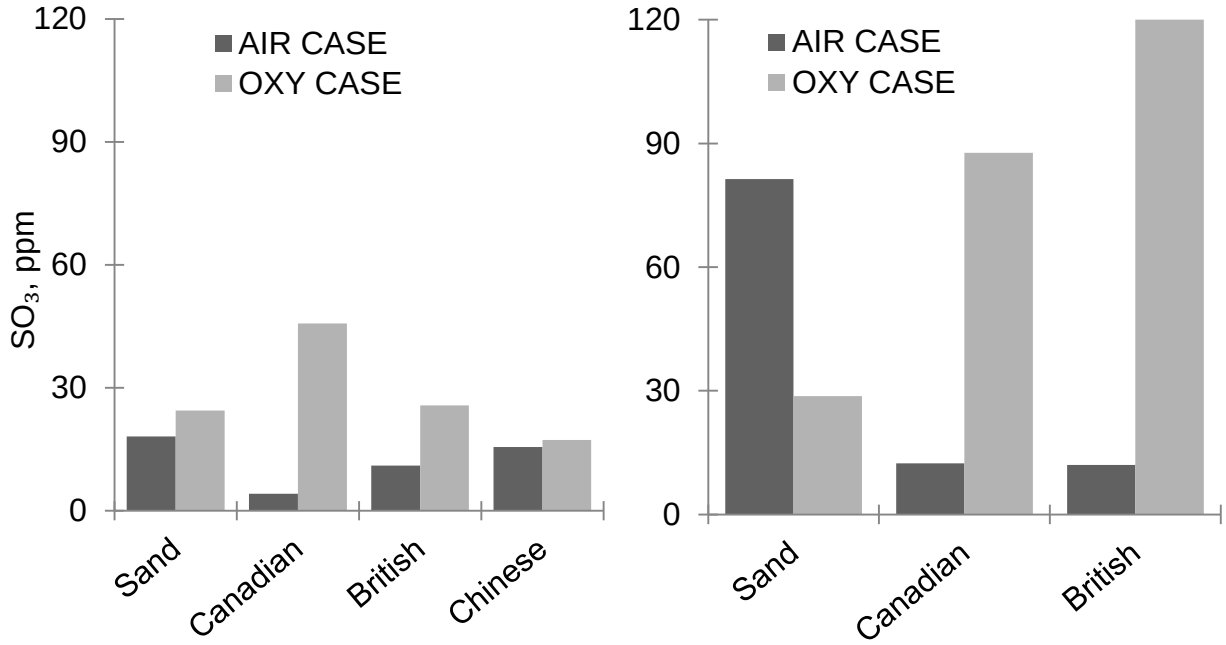
The catalytic effect of fly ashes on SO_3 formation is presented in Figs. 10 and 11, and can be explored by comparison with the sand case. Fig. 10 shows experimental results with 1000 and 4000 ppm of inlet SO_2 concentration at 400°C. A stronger effect on SO_3 formation was seen with British fly ash, with formation of 8 ppm and over 10 ppm under air and oxy-fuel environments, respectively. At a 1000 ppm at 400°C, there is possibly a weak catalytic effect for the Canadian ash, although it should be remembered that experimental error is within 1-2 ppm. At 4000 ppm, however, the British fly ash clearly shows a strong catalytic effect at 400°C as compared with sand. At 950°C, Fig. 11 shows that there appears to be a strong catalytic effect under oxy-firing conditions for the Canadian and British ashes, and

this situation is more pronounced for both these two ashes at the 4000 ppm SO_2 level.



(a) SO_2-1000 ppm (b) SO_2-4000 ppm

Fig. 10. Catalytic effect of ashes on SO_3 formation at 400°C



(a) SO_2-1000 ppm (b) SO_2-4000 ppm

Fig.11. Catalytic effect of ashes on SO_3 formation at 950°C

4. Conclusions

Low- and high-temperature experiments were conducted to investigate sand- and fly ash-catalysed formation of SO_3 in a bench-scale bubbling fluidised bed under air and oxy-fuel combustion environments. Two temperatures were chosen, namely 400°C to represent the formation of SO_3 at the back end of the combustion furnace and 950°C to represents the environment in the fluidised bed. Here, the formation of SO_3 is favoured under oxy-fuel combustion conditions when compared to air combustion conditions for all the fly ashes at 950ºC. At 400ºC the situation is more complicated and depends both on the ash and the SO_2 concentrations, but clearly catalysis to form SO_3 is occurring even at this low temperature, albeit that the sand is often as or more effective than the fly ash at catalysing SO_3 production, which may mean other factors such as the carbon content of the fly ashes for instance are reducing any catalytic effect associated with fly ash at the low temperature condition. Higher concentrations of SO_2 also favour the formation of SO_3, at 400°C.

XRF analyses clearly indicated that some sulphation of the metal oxides in the ash occurred at both temperatures and this too must impact on SO_3 levels, although any reduction in SO_3 levels due to ash sulphation would probably be better described as capture. However, the ash with the least alkaline earth materials (namely the British ash) is clearly the most effective catalyst at low temperatures, and among the most effective in catalysing SO_3 formation at high temperatures, so any such effect must be secondary.

Acknowledgements

The authors would like to acknowledge Dr Kumar Patchigolla for supplying the British fly ashes used in these experiments, for useful discussions on the operation of the experimental rig and for discussing appropriate safety precautions. The authors also wish to thank Dr Nelia Jurado for useful discussion on the measurements and analysis methods for SO_3. The financial support for the PhD program from Nazarbayev University is also gratefully acknowledged.

References

[1] M.B. Toftegaard, J. Brix, P.A. Jensen, P. Glarborg, A.D. Jensen, Oxy-fuel combustion of solid fuels, Prog. Energy Combust. Sci. 36 (2010) 581–625.

[2] T. Wall, Y. Liu, C. Spero, L. Elliott, S. Khare, R. Rathnam, F. Zeenathal, B. Moghtaderi, B. Buhre, C. Sheng, R. Gupta, T. Yamada, K. Makino, J. Yu, An overview on oxyfuel coal combustion—State of the art research and technology development, Chem. Eng. Res. Des. 87 (2009) 1003–1016.

[3] B.J.P. Buhre, L.K. Elliott, C.D. Sheng, R.P. Gupta, T.F. Wall, Oxy-fuel combustion technology for coal-fired power generation, Prog. Energy Combust. Sci. 31 (2005) 283–307.

[4] H. Liu, Y. Shao, Predictions of the impurities in the CO_2 stream of an oxy-coal combustion plant, Appl. Energy. 87 (2010) 3162–3170.

[5] E. Croiset, K.V. Thambimuthu, NO_x and SO_2 emissions from O_2/CO_2 recycle coal combustion, Fuel. 80 (2001) 2117–2121.

[6] E. Croiset, C. Heurtebise, J.P. Rouan, J.R. Richard, Influence of pressure on the heterogeneous formation of nitrogen oxides during char combustion, Combust. Flame. 112 (1998) 33–44.

[7] R.E. Moser, Benefits of Effective SO_3 Removal in Coal-Fired Power Plants: Beyond Opacity Control, In: Power Plant Air Pollution Control Mega Symposium, Baltimore MD, 2006.

[8] Y. Cao, H. Zhou, W. Jiang, C.W. Chen, W.P. Pan, Studies of the fate of sulfur trioxide in coal-fired utility boilers based on modified selected condensation methods, Environ. Sci. Technol. 44 (2010) 3429–3434.

[9] Y. Tan, E. Croiset, M.A. Douglas, K.V. Thambimuthu, Combustion characteristics of coal in a mixture of oxygen and recycled flue gas, Fuel. 85 (2006) 507–512.

[10] C.F. Cullis, M.F.R. Mulcahy, The kinetics of combustion of gaseous sulphur compounds, Combust. Flame. 18 (1972) 225–292.

[11] N.A. Burdett, W.E. Langdon, R.T. Squires, Rate coefficients for the reaction $SO_2 + O_2 = SO_3 + O$ in the temperature range 900-1350 K, Inst. Energy. 57 (1984) 373–376.

[12] M.U. Alzueta, R. Bilbao, P. Glarborg, Inhibition and sensitization of fuel oxidation by SO_2, Combust. Flame. 127 (2001) 2234–2251.

[13] R.E. Barret, J.D. Hummell, W.T. Reid, Formation of SO_3 in a noncatalytic combustor, J. Eng. Power, Trans. ASME. 88 (1966) 165–172.

[14] D. Flint, A.W. Lindsay, Catalytic oxidation of sulphur dioxide on heated quartz surfaces, Fuel. 30 (1951) 288.

[15] L.P. Belo, L.K. Elliott, R.J. Stanger, R. Spörl, K.V. Shah, J. Maier, T.F. Wall, High-temperature conversion of SO_2 to SO_3: homogeneous experiments and catalytic effect of fly ash from air and oxy-fuel firing, Energy Fuels. 28 (2014) 7243–7251.

[16] D. Fleig, M.U. Alzueta, F. Normann, M. Abián, K. Andersson, F. Johnsson, Measurement and modeling of sulfur trioxide formation in a flow reactor under post-flame conditions, Combust. Flame. 160 (2013) 1142–1151.
[17] L. Duan, Y. Duan, Y. Sarbassov, Y. Li, E.J. Anthony, SO_3 formation under oxy-CFB combustion conditions, Int. J. Greenh. Gas Control. 43 (2015) 172–178.
[18] X. Wang, X. Liu, D. Li, Y. Zhang, M. Xu, Effect of steam and sulfur dioxide on sulfur trioxide formation during oxy-fuel combustion, Int. J. Greenh. Gas Control. 4 (2015) 1–9.
[19] J. Ahn, R. Okerlund, A. Fry, E.G. Eddings, Sulfur trioxide formation during oxy-coal combustion, Int. J. Greenh. Gas Control. 5 (2011) S127-S135.
[20] R. Spörl, J. Walker, L. Belo, K. Shah, R. Stanger, J. Maier, T. Wall, G. Scheffknecht, SO_3 emissions and removal by ash in coal-fired oxy-fuel combustion, Energy and Fuels. 28 (2014) 5296–5306.
[21] R. Spörl, J. Maier, G. Scheffknecht, Experiences and Results of SO_3 Measurements Performed under Oxy-Coal Fired Conditions, in: IEAGHG, Special Workshop on SO_2/SO_3/Hg and Corrosion Issues in Oxyfuel Combustion Boiler and Flue Gas Processing Units, London, Jan. 25-26, 2011.
[22] D. Fleig, K. Andersson, F. Johnsson, Influence of operating conditions on SO_3 formation during air and oxy-Fuel combustion, Ind. Eng. Chem. Res. 51 (2012) 9483–9491.
[23] E.G. Eddings, L. Wang, J. Ahn, Bench-scale fluid bed experiments of SO_2/SO_3 formation and sulfur capture in N_2/O_2 and CO_2/O_2 environments, in: IEAGHG Special Workshop on SO_2/SO_3/Hg and Corrosion Issues in Oxyfuel Combustion Boiler and Flue Gas Processing Units, London, Jan. 25-26,2011.
[24] P. Marier, H.P. Dibbst, The catalytic conversion of SO_2 to SO_3 by fly ash and the capture of SO_2 and SO_3 by CaO and MgO, Thermochim. Acta. 8 (1974) 155–165.
[25] J.S. Dennis, A.N. Hayhurst, The formation of SO_3 in a fiuidized bed, Combust. Flame. 72 (1988) 241–258.
[26] R.F. Maddalone, S.F. Newton, R.G. Rhudy, R.M. Statnick, Laboratory and field evaluation of the controlled condensation system for SO_3 measurements in flue gas streams, J. Air Pollut. Control Assoc. 29 (1979) 626–631.
[27] L. Duan, H. Sun, C. Zhao, W. Zhou, X. Chen, Coal combustion characteristics on an oxy-fuel circulating fluidized bed combustor with warm flue gas recycle, Fuel. (2014) 47-51.
[28] D. Kunii, O. Levenspiel, Fluidization Engineering, second ed. Butterworth-Heinemann, Stoneham, 1991.
[29] R.J. Jaworowski, S.S. Mack, Evaluation of methods for measurements of SO_3/H_2SO_4 in flue gas, J. Air Pollut. Control Assoc. 29 (1979) 43–46.
[30] D. Fleig, E. Vainio, K. Andersson, A. Brink, F. Johnsson, M. Hupa, Evaluation of SO_3 measurement techniques in air and oxy-fuel combustion, Energy Fuels. 26 (2012) 5537–5549.

[31] Chemical equilibrium calculation, Colorado State University, Available at: http://navier.engr.colostate.edu/~dandy/code/code-4/index.html, 2016 (accessed 02.04.16).



https://dspace.org/

SO3 formation and the effect of fly ash in a bubbling fluidised bed under oxy-fuel combustion conditions

Sarbassov, Yerbol; Duan, Lunbo; Jeremias, Michal; Manovic, Vasilije; Anthony, Edward J.

2017-07-18
Elsevier
http://dx.doi.org/10.1016/j.fuproc.2017.07.015
Sarbassov Y, Duan L, Jeremias M, Manovic V, Anthony EJ, SO3 formation and the effect of fly ash in a bubbling fluidised bed under oxy-fuel combustion conditions, Fuel Processing Technology, Vol. 167, December 2017, pp. 314-321

Downloaded from a DSpace repository. https://dspace.org/